

FLASH: Fast All-to-All Communication in GPU Clusters

Yiran Lei
Carnegie Mellon University
yiranlei@cs.cmu.edu

Daniar Kurniawan
MangoBoost Inc.
daniar.kurniawan@mangoboots.io

Changsu Kim
MangoBoost Inc.
changsukim@mangoboots.io

Arvind Krishnamurthy
University of Washington
arvind@cs.washington.edu

Dongjoo Lee
MangoBoost Inc.
dongjoo.lee@mangoboots.io

Chanmyeong Kim
MangoBoost Inc.
chanmyeong.kim@mangoboots.io

Hyeonseong Choi
MangoBoost Inc.
hyeonseong.choi@mangoboots.io

Justine Sherry
Carnegie Mellon University
sherry@cs.cmu.edu

Liangyu Zhao
University of Washington
liangyu@cs.washington.edu

Heetaek Jeong
MangoBoost Inc.
heetaek.jeong@mangoboots.io

Liangcheng Yu
University of Pennsylvania
leoyu@seas.upenn.edu

Eriko Nurvitadhi
MangoBoost Inc.
eriko@mangoboots.io

Abstract

Scheduling All-to-All communications efficiently is fundamental to minimizing job completion times in distributed systems. Incast and straggler flows can slow down All-to-All transfers; and GPU clusters bring additional straggler challenges due to highly heterogeneous link capacities between technologies like NVLink and Ethernet. Existing schedulers all suffer high overheads relative to theoretically optimal transfers. Classical, simple scheduling algorithms such as SpreadOut fail to minimize transfer completion times; modern optimization-based schedulers such as TACCL achieve better completion times but with computation times that can be orders of magnitude longer than the transfer itself.

This paper presents FLASH, which schedules near-optimal All-to-All transfers with a simple, polynomial time algorithm. FLASH keeps the bottleneck inter-server network maximally utilized and, in the background, shuffles data between GPUs over fast intra-server networks to mitigate stragglers. We prove that, so long as intra-server networks are significantly faster than inter-server networks, FLASH approaches near-optimal transfer completion times. We implement FLASH and demonstrate that its computational overheads are negligible, yet it achieves transfer completion times that are comparable to state-of-the-art solver-based schedulers.

1 Introduction

Collective communications – in which a cluster of compute nodes must exchange data simultaneously – are heavily used in high-performance computing (HPC) and distributed machine learning (ML). All-to-All communication is a form of collective communication in which every compute node may transmit to every other node. In modern GPU clusters, each node is a GPU within a server, and GPUs are connected via

intra-server networks (e.g., NVLink) and inter-server networks (e.g., Ethernet, Infiniband). In HPC, All-to-All is used between GPUs for Fast Fourier Transforms (FFT) [40], e.g., in molecular dynamics [11] and direct numerical simulations [30]. In distributed machine learning (ML), All-to-All between GPUs appears in Deep Learning Recommendation Models (DLRM) [31, 32] and mixture-of-expert (MoE) models [26, 44]. Unfortunately, All-to-All communication is often a performance bottleneck at scale [9, 24, 26, 43]: studies show that ML training can spend 40–56.7% of runtime in All-to-All transfers [24, 31], and in scientific computing 3D FFTs can spend up to 97% of runtime in network transfer [9]!

Efficiently executing All-to-All transfers is challenging due to two familiar demons from the networking literature: *incast* and *stragglers*. Incast occurs when multiple network flows target the same receiver, leading to queueing delays, packet loss, and inefficient link utilization [17, 23, 50, 51]. To avoid incast, *schedulers* carefully plan out sequences of pairwise transfers to guarantee that each receiver accepts a single flow at a time. Unfortunately, scheduling is plagued by *stragglers*: transfers that take significantly longer to complete than other pairwise transfers scheduled to occur at the same time. Waiting for these ‘straggling’ transfers to complete before allowing new pairwise transfers to start leaves most of the network idle when it could be working to transmit new data.

Stragglers often occur when pairwise transfer sizes are *skewed* and some flows must transfer significantly more data than others. However, in GPU clusters, stragglers are also problematic balanced workloads due to *heterogeneous link capacities*. Intra-server networks such as NVLink offer 7200Gbps of capacity between GPUs, but inter-server networks offer only 400Gbps of capacity. Hence, even pairwise

transfers of the same size may differ in flow completion time (FCT) by orders of magnitude depending upon how they are routed.

Today’s All-to-All schedulers are plagued by incast and stragglers. Classical algorithms such as FanOut [7] and Spread-Out [33] are simple approaches to scheduling that take 2.5–91× longer to complete All-to-All transfers than a theoretical optimum (§6). A modern line of research (such as TE-CCL [29] and TACCL [48]) uses computationally complex algorithms to compute optimized schedules; the transfers they compute for balanced workloads (*i.e.*, those without skew) complete near-optimally. However, the time to compute one schedule ranges from minutes to days, all for an All-to-All transfer, which itself completes in milliseconds! Making matters worse, to remain tractable, modern algorithms do not encode workload skew at all, which we also observed to be common in the workloads we studied.

Hence, our key research question is as follows: *Is it possible to design an All-to-All scheduling algorithm for GPU clusters that defeats incast and stragglers, while also computing schedules quickly?*

In this paper, we present FLASH, a fast, near-optimal scheduler for All-to-All transfers in modern GPU clusters. The key insight behind FLASH is to take advantage of a key property of all ML-optimized architectures we are aware of: they contain one inter-server network, and a set of intra-server networks which is at least an order-of-magnitude faster than the inter-server network. FLASH prevents stragglers by using the fast intra-server networks to load balance and shuffle data within servers. By shuffling/load balancing data *within* servers, FLASH can keep the bottleneck inter-network links *maximally utilized*, guaranteeing that the limiting resource is *always* occupied. Like prior work, FLASH ensures that the schedule avoids incast by only allowing one transfer per receiver at a time; FLASH achieves this by borrowing an algorithm called Birkhoff’s Decomposition [12], used in router port scheduling [15, 28], which we discuss in §4.2.

FLASH is near-optimal; in simulations, we show that the overhead of FLASH relative to a theoretical optimum is, in practice, small. We prove that as the ratio between intra-server bandwidth and inter-server bandwidth grows, FLASH’s overhead relative to optimal shrinks proportionally. We incorporate FLASH into the Megatron-LM [49] MoE library on a 4-node cluster with 32 AMD MI300X GPUs. With FLASH, end-to-end training runs 4.48× faster than the same workload using the baseline RCCL [8] library. Furthermore, FLASH generates transfer completion times for balanced workloads that are comparable to optimal schedulers such as TACCL, even though FLASH computes its schedule in 32 microseconds while TACCL consumes an hour in its own computation.

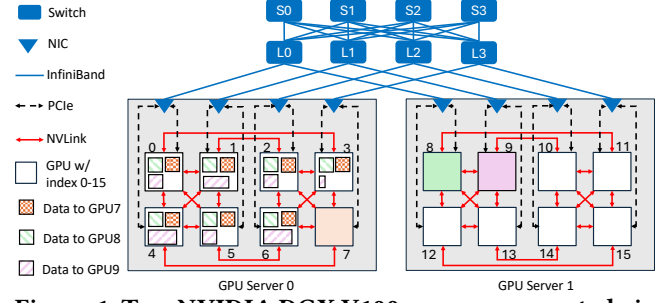


Figure 1: Two NVIDIA DGX V100 servers connected via the Rail-optimized topology [13]: blue/red lines show the inter-/intra- server network. It also shows partial All-to-All workload: from GPU 0-6 to GPU 7-9.

The rest of this paper is organized as follows: in §2 we motivate the need to optimize the skewed and dynamic All-to-All transfer for ML workloads and introduce the issues of prior work and our insight; in §3 and §4, we introduce a two-tiered scheduling algorithm and prove a bound overhead relative to the theoretical optimum; we integrate FLASH into a MoE training system in §5, evaluate FLASH in §6, and discuss related prior work in §7.

2 Motivation

Implementations of All-to-All schedulers were embedded in MPI [41] as early as the 1990’s. Since then, All-to-All has been explored in the context of high-performance computing (HPC) [10, 42], in ‘big data’ datacenter workloads as a form of ‘coflow’ [16], and today is an important communication pattern in machine-learning optimized GPU clusters [21, 22, 26]. Studies show that All-to-All can consume 40–56.7% of runtime in machine learning workloads for Mixture-of-Expert (MoE) [26] and DLRM [31] machine learning models; in the context of 3D Fast Fourier Transforms [9] All-to-All transfers consume up to 97.3% of runtime!

Modern GPU clusters add new complexity to the All-to-All problem. Figure 1 illustrates an ML-optimized cluster of DGX V100 servers. Logically, each sender/receiver is not a server but, instead, a GPU within a server. Each GPU is connected to two networks. First, there is a PCIe network, which in turn connects to a NIC and an inter-server network running, *e.g.*, Ethernet or Infiniband, with approximately 100Gbps of bandwidth per link. Second, there is an intra-server network connecting GPUs within the same server using an interconnect like NVLink [6], which offers 150GBps (1200Gbps) per link. This path diversity leads to many routing choices: a transfer from GPU 5 to GPU 7 within Server 0 in Figure 1 might go *either* over NVLink by waypointing through another GPU or over Ethernet, routing through two NICs and a ToR switch. This is just one of *many* deployed configurations; *e.g.*, the AMD MI300X [2] uses a fully connected mesh for

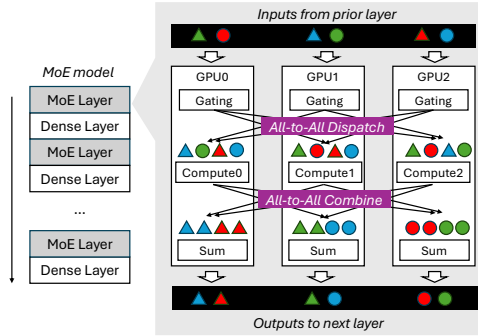


Figure 2: MoE model structure: a stack of alternating MoE layers and dense transformer layers; All-to-All communications (marked in purple) happen twice at every MoE layer.

the intra-server network, and the NVIDIA H100 [36] uses a switch. Hence, a routing strategy designed for one particular GPU cluster may not generalize to others.

As a running, state-of-the-art example, we explore a particular ML workload deployed on GPUs today called Megatron-LM [49], a Mixture-of-Expert (MoE) model. MoE architectures are currently in vogue in natural language processing (NLP) as a MoE model called DeepSeek-V3 [19] outperformed the well-known GPT-4o [38] in six benchmark tests. MoE models have other successful applications in computer vision [45] and reinforcement learning [37]. The key idea behind MoE is to use multiple small neural networks called ‘experts’, each trained to focus on a different subset of the dataset. Then, a gating network at runtime determines which experts should be activated for a specific input. In implementation, typically, each GPU hosts an expert. As shown in Figure 2, All-to-All communication is frequently called in MoE models: it happens **twice** at **every** MoE layer while typically **half** of the entire model is MoE layers. Prior work has reported All-to-All communication can take 56.7% of the total runtime [24].

During inference, each MoE layer has two All-to-All transfers. The first All-to-All transfer dispatches the inputs that are randomly scattered among the experts to the activated experts based on the decisions from the gating network; the second combines the computation outputs when each input activates more than one expert. During training, there are similarly two corresponding All-to-All communications in the backward propagation pass. Each All-to-All transfer in inference or training has a unique traffic matrix: the sizes of transfers and the selected experts vary based on the input data.

2.1 All-to-All Schedulers

As discussed previously, existing schedulers for All-to-All transfers fall into two camps: computationally fast, ‘classical’

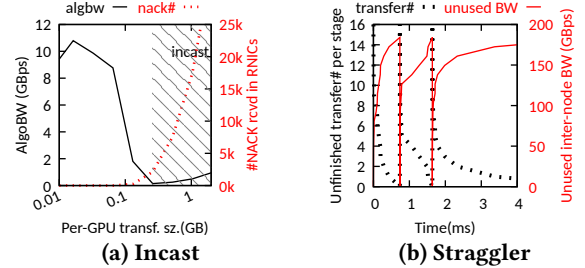


Figure 3: Incast and straggler effects when using FanOut (no scheduling) and SpreadOut algorithm for All-to-All.

approaches that offer far from optimal transfer times, and computationally expensive ‘optimal’ approaches that offer fast transfers at the cost of high compute times. The key challenges all of these algorithms are trying to resolve are *incast* and *stragglers*.

To understand the impact of incast and stragglers, we measure their impact on transfer efficiency. The figure of merit for scheduler efficiency is a metric called ‘algorithmic bandwidth’, which is the *total amount of data to be transferred* (S) divided by the time to complete the transfer (t) and the number of GPUs participating in the All-to-All transfer (N), $AlgoBW = S/t/N$ [29, 48]. The higher the AlgoBW, the faster an All-to-All transfer can be completed.

The incast effect: The simplest scheduler is simply to allow all GPUs to transfer simultaneously with multiple parallel connections between each sender/receiver (FanOut [7]). This approach leads to poor performance because of *incast*: multiple connections sharing the same link fill up link buffers, leading to high packet loss, low throughput, and high latency [50, 51]. With too many competing, simultaneous transfers, overall goodput is low and many packets are retransmitted. In Figure 3a, we run an experiment in which 32 GPUs from 4 nodes, connected to the same ToR switch, do an All-to-All transfer. We see that for transfers of any more than a few hundred megabytes, loss rates increase and AlgoBW plummets.

The SpreadOut [33] algorithm was designed to avoid inefficiencies due to network contention. The key idea behind SpreadOut is to *stage* transmissions so that each sender and each receiver are involved in at most one connection at a time.

The straggler effect: Although SpreadOut avoids inefficiency due to network contention, it suffers from *stragglers*: a phenomenon where most pairwise transfers complete, but a few lengthy transfers continue for a much longer period of time. Since most pairwise transfers have completed, the majority of the network capacity remains idle. However,

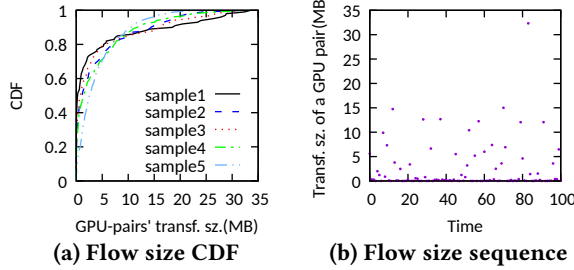


Figure 4: All-to-All workload is unbalanced and dynamic when training Megatron-LM MoE model.

new transfers cannot start to use this idle capacity until the ‘straggling’ pairs complete.

One reason that stragglers appear in GPU clusters is due to the heterogeneous link speeds at play: flows transferred over the intra-server network will complete significantly faster than similarly-sized flows transferred across the inter-server network.

Even with homogeneous link capacities, however, stragglers can arise due to *skewed workloads* in which some pairs have more data to transfer than others and simply take longer to complete. In MoE workloads, such skewness is common. We ran the Megatron-LM MoE model [49] in a 4-node cluster with 32 experts and measured pairwise flow sizes for the first 10,000 iterations of All-to-All transfers. Figure 4a shows significant skew in five sample transfers; a 90th percentile flow is roughly 12.5 \times larger than a median flow.

We see how straggler effects lead to resource underutilization in Figure 3b. Here, we perform a 2-node All-to-All transfer that follows the distribution of Megatron-LM MoE training workload using SpreadOut and measure the number of active flows of each stage (on y1) and the amount of unused inter-node bandwidth (shown on y2) over time. The amount of unused inter-node bandwidth rapidly increases over time as individual flows complete, and as a result, most inter-node links remain idle most of the time, simply waiting for the current stage to end so that new transfers can begin.

Trading off computation for network optimality: The newest schedulers explicitly target heterogeneous GPU clusters. These schedulers include TE-CCL [29] and TACCL [48]. Like SpreadOut, they all avoid incast by guaranteeing at most one flow per sender/receiver at a time. However, unlike SpreadOut, they do not explicitly coordinate rounds or stages of computation. Instead, the tool computes a schedule that is aware of variable flow finishing times due to heterogeneous link capacity and may stage multiple shorter flows while a longer flow completes.

To compute a schedule, these tools use constraint-based programming tools like mixed integer linear programming (MILP) or reductions to multi-commodity flow problems. The input to the schedule includes the network topology,

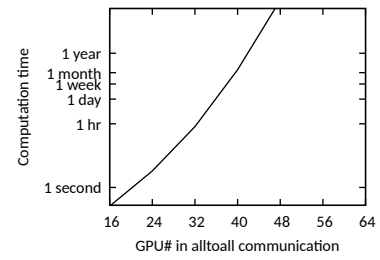


Figure 5: Computation time required by state-of-the-art scheduling work (TACCL).

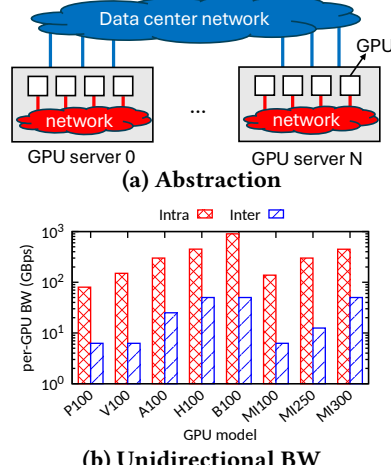


Figure 6: Modern GPU cluster can be abstracted as fast network at small scale (i.e., intra-node) and slow network at large scale (i.e., inter-node).

bandwidths, and the traffic matrix. To maintain tractability, they assume that workloads are *balanced*, with all pairwise flows of the same size, rather than *skewed*. Nonetheless, the state-of-the-art scheduler, TACCL, still takes on the order of minutes or weeks (depending on the scale of the cluster) to compute an optimal schedule. We illustrate TACCL’s runtime as cluster size scales in Figure 5.

High scheduler runtime means that TACCL and similar solutions are only suitable for workloads where there is no skew and where the *same* traffic matrix appears over and over. Since a typical transfer completes in milliseconds, a schedule computation of minutes does not help anything unless the computation cost is amortized over a series of many transfers, each with the same structure. Unfortunately, not only do MoE workloads exhibit skew, but they are also highly dynamic. The All-to-All workload in MoE [26, 31] is model-input-dependent and can change at the time scale of seconds. In Figure 4b, we see the sequence of pairwise transfer sizes for a single pair of GPUs over time in our Megatron-LM MoE training experiment: each iteration involves a different size of transferred data, illustrating how the weights of the traffic matrix change with each round.

2.2 FLASH

Our goal in designing FLASH is to develop a new, straggler-avoidant approach to scheduling in GPU clusters despite skew and dynamic workloads. FLASH simplifies the model of GPU clusters by simply assuming that the GPU cluster has one ‘slow’ network, which is the bottleneck resource for data transfer, and a collection of ‘very fast’ networks between GPUs. We illustrate this model in Figure 6a. Comparing to the DGX V100 figure in Figure 1, the PCIe and Ethernet connectivity have been subsumed into one ‘datacenter network’ and the NVLink networks are now the smaller ‘GPU networks’ as shown. Figure 6b compares the intra-server bandwidth and inter-server bandwidth for a range of GPU-optimized clusters. Although bandwidths themselves vary from architecture to architecture, the trend of a roughly 10× difference between intra- and inter-server bandwidths holds strong.

FLASH uses the intra-server networks to load balance data within each server (§4.1) The inter-server network is scheduled to transfer data in rounds such that no receiver experiences incast, much like SpreadOut (§4.2). Together, these approaches guarantee that the server with the most data to send (or receive) has uplinks (or downlinks) that are fully utilized and never idle. FLASH’s staging introduces a small overhead relative to a theoretical optimal approach, but we show that this overhead is, in practice, small and decreases proportionally to the ratio of bandwidth between intra- and inter-server links (§4.4). In the next few sections, we present FLASH’s design in detail.

3 Design Overview

To build a lightweight yet near-optimal scheduler for unbalanced All-to-All communication in modern GPU clusters, FLASH is driven by two overarching design principles:

1. Maximize inter-server bandwidth utilization.
2. Exploit intra-server networks to balance and optimize inter-server workloads.

The first principle arises from the fact that inter-server bandwidth is the primary bottleneck in All-to-All communication. Since most transfers cross servers and inter-server links are significantly slower than intra-server links, treating all links equally underutilizes inter-server capacity, leading to stragglers that degrade performance. Instead, FLASH prioritizes inter-server links, ensuring their bandwidth is fully utilized.

To achieve this, FLASH harnesses fast intra-server links to balance workloads before and after data crosses the inter-server fabric boundary. Rather than leaving intra-server bandwidth idle, FLASH proactively shuffles data within a server, preventing overloading of any single inter-server link. By allowing multiple GPUs to assist in load balancing and

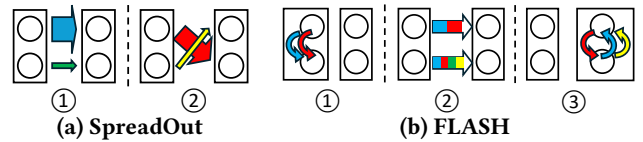


Figure 7: All-to-All transfer process in a 2x2 cluster: SpreadOut is slowed by the straggler (wide arrow) at each step while FLASH balances load, sends equal-size data over inter-node links, and redistributes data to destination GPUs.

data offloading, FLASH minimizes stragglers and maximizes throughput.

Combined, this tiered network view transforms All-to-All scheduling from a black-box problem into a structured optimization, enabling efficient and scalable schedule computations. We formally prove FLASH’s optimality in §4.4.

In addition, FLASH also handles incast—a well-known issue in AI workloads [17], particularly for RDMA networks [23]. By ensuring that each receiver communicates with only one sender at a time, FLASH significantly reduces congestion.

FLASH is designed with assumptions that align with most modern deployments: (1) Uniform GPU uplink/downlink bandwidth interfacing the inter-server fabric; (2) Symmetric configurations of NICs and GPUs for each server (as seen in DGX and MI300X clusters); and (3) Dedicated network environment, where All-to-All communication is the primary source of congestion. We leave support for heterogeneous devices and shared environments as future work.

4 Two-Tiered Scheduling

In this section, we introduce FLASH with a simple example including only two servers §4.1. We then generalize the approach to multiple servers in §4.2 and then present one final pipelining optimization to reduce FLASH’s completion time even further in §4.3. Finally, we provide a formal analysis of FLASH quantifying its modest overheads relative to a theoretical optimal approach (§4.4).

4.1 Two Server Example

Even in a simple setting with only two servers, incast can be a problem when multiple GPUs from one server transmit to the same receiving GPU on the other server. To avoid incast, we must let any receiver GPU have at most one sender GPU at a time. The baseline SpreadOut algorithm [33] satisfies this requirement by staging transfers. Figure 7a illustrates the SpreadOut algorithm: each receiving GPU (circle) only receives from one sender and transmission is staged across two phases.. Unfortunately, in the example shown, there is *skew* in the transfer - with some larger transfers than others. Hence, the small transfer (thin arrow) is forced to wait for the

large transfer (wide arrow) to complete while inter-server bandwidth between them sits idle.

FLASH counter-intuitively uses three stages rather than two to nonetheless achieve a faster end to end All-to-All transfer completion time. As shown in Figure 7b, FLASH schedules the unbalanced All-to-All transfer in three steps: **Step 1: Load balance.** Before the inter-server transfers, we shuffle all the data within the sending server to equalize the amount of data on each GPU. This operation is implemented by an intra-node All-to-All communication as shown by the curve arrows in Figure 7b. Because this All-to-All operation occurs entirely over the fast intra-server network, it has an almost-negligible completion time relative to a transfer over the inter-server network..

Step 2: Merged transfer. Each GPU transmits *all of its data* to one GPU on the receiving server as shown in Figure 7b. Some of the data may not be destined for the receiving GPU, but the data is still making progress towards its final destination. After this step, all of the data will be on the correct *server*, although not necessarily on the correct GPU. Because the data has been load balanced, this step completes more quickly than either stages one or two in the SpreadOut example and there is no link idle time.

Step 3: Redistribute. Now that all of the data is on the correct server, FLASH redistributes the data between GPUs on the same server so that all of the data is on the correct GPU. Once again, this is an intra-server All-to-All operation, and hence it has an almost negligible completion time relative to a transfer over the inter-server network.

Although FLASH can introduce extra phases of transfer relative to SpreadOut, it typically performs well because it improves AlgBW over the bottleneck inter-server network: no link is ever idle between the pair of servers because the workload has been balanced. The additional costs due to load balancing and redistribution are relatively small because of the high bandwidth of the intra-server interconnect.

This example summarizes FLASH; in the next two sections we generalize the above algorithm to a multi-server setting and then demonstrate how to additionally hide the (small) latency from load balancing and distribution by pipelining transfer stages.

4.2 Multi-Server Scheduling

The previous section shows how FLASH balances GPU-to-GPU transfers between servers. However, in larger clusters, each server may contain data destined for GPUs on *multiple* servers. This introduces a new source of skew or imbalance: server A might have 100MB to send to server B and 50MB for server C, while Server B might have 25MB for server A and 75MB for server C, etc. Figure 8 shows two examples with

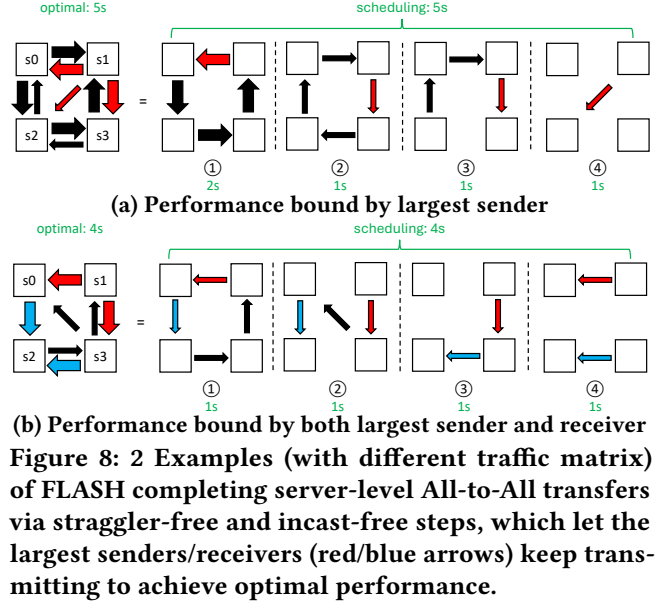


Figure 8: 2 Examples (with different traffic matrix) of FLASH completing server-level All-to-All transfers via straggler-free and incast-free steps, which let the largest senders/receivers (red/blue arrows) keep transmitting to achieve optimal performance.

four servers each. Some pairs of servers have large amounts of data to transfer, others have little or none.

Once again, our goal is to develop a schedule such that (a) each sender/receiver is involved in at most one transfer at once to avoid incast, (b) the bottleneck senders and receivers are *continuously occupied* thus guaranteeing optimal All-to-All completion.

Approach: FLASH leverages Birkhoff's Theorem [12] to achieve these goals; the same approach has been adopted in router architectures to similar ends but to the best of our knowledge this is its first application to GPU All-to-All. Birkhoff decomposes an imbalanced traffic matrix into a sum of smaller, balanced traffic matrices such that each transfer within a given matrix is of the same size. Longer flows may be broken up into a series of smaller, shorter flows. Figure 8 shows how FLASH might decompose the two sets of imbalanced transfers into a sequence of balanced stages, guaranteeing straggler-freedom within a stage.

Although some server-pairs spend some stages with their links idle, the *bottleneck* servers (those with the most data to send/receive) are continuously occupied, guaranteeing a minimal completion time. For example, the All-to-All workload shown in Figure 8a is bound by the largest sender s_1 which needs at least 5s to send all its data to every receiver; hence s_1 transmits in all four stages while other servers complete earlier.

Number of stages: Although Birkhoff's theorem guarantees us a minimal completion time in *theory*, in practice FLASH introduces some overhead with the orchestration of each stage (e.g., to open up new connections at each stage). This static overhead is negligible under large transfer sizes

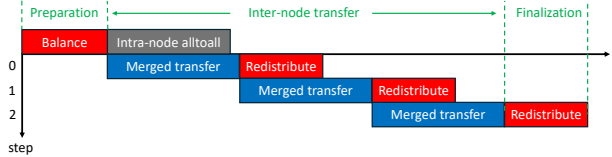


Figure 9: FLASH pipelines consecutive transfer steps: the current step’s intra-node (red) data-redistribution is executed concurrently with the next step’s inter-node (blue) transfer.

but can be observed with small transfers. Reducing the number of transfer steps mitigates this issue, however, decomposing an arbitrary All-to-All workload into the *minimal* number of straggler-free and incast-free steps is an NP-hard problem [20].

Scheduling complexity: The computation complexity is $O(\text{server}^{\#5})$, which is a lower order of complexity than prior work [14, 35]’s SMT or MILP solver. In practice, computation time is generally small in a modern CPU, less than 1 ms when $\text{server}^{\#} < 10$ and less than 0.25 s when $\text{server}^{\#} < 50$.

4.3 FLASH Transfer Pipeline

We now combine the techniques introduced in prior sections and introduce the complete scheduling algorithm. Suppose there are n servers and m GPUs at each server that participate in the All-to-All transfer. As shown in Figure 9, FLASH includes three transfer stages, i.e., preparation, inter-node transfer, and finalization.

In the beginning, each GPU in the system has some arbitrary amount of data planned to be sent to every other GPU. In the preparation stage, FLASH does load balancing for inter-server transfers. All the cross-node data that has the same destination server is balanced among m GPUs. Each server does $(n - 1)$ times load balancing for $(n - 1)$ other servers in the system. When the preparation stage finishes, for any source and destination server pair, all the GPUs from the source server have an equal amount of data for the destination. So, the transfer size from one server to another can be represented by a single number, reducing the initial GPU-level All-to-All workload to a server-level All-to-All workload.

Then comes the inter-node transfer stage, which constitutes the majority of the transfer process. FLASH uses the Birkhoff’s Theorem to decompose the server-level All-to-All workload into a series of straggler-free and incast-free transfer steps, e.g., 3 steps in Figure 9. At each step, a server sends a specific amount of data to a receiving server using the inter-server network or simply stays idle. When sending data, all the GPUs of the sending server communicate with their peer GPUs at the receiving server. Thus, GPU i at the sender side only talks to GPU i at the receiver side and transmits one

data chunk, which is the current step’s transfer size. After the inter-server transfer, the GPUs at the receiving server redistribute the misplaced data to their actual destination GPUs, which is an intra-node All-to-All communication. To improve performance, FLASH pipelines consecutive transfer steps such that the current step’s intra-node data redistribution is executed concurrently with the next step’s inter-server transfer. Finally, FLASH handles the transfers that do not need to cross the servers, i.e., the intra-node part of the All-to-All workload, and executes it concurrently with the first step’s inter-node transfer as shown by the grey block in Figure 9.

The finalization stage is the pipeline tail which is the data redistribution of the last transfer step. The transfer pipeline shown in Figure 9 can achieve near-optimal performance: the time of the inter-node transfer stage is close to the theoretical lower bound, because Birkhoff’s Theorem maximizes the bottleneck performance by ensuring that the largest senders or receivers are never idle. The performance sub-optimality comes from the pipeline head (initial load balancing) and tail (final data redistribution), which we later prove can be negligible given a fast-enough intra-node network.

4.4 Optimality Bound

In this section, we prove a performance bound between FLASH and theoretical optimality.

We first introduce the symbols and assumptions used for proofs. We denote the bandwidth of intra-server and inter-server links as B_1 and B_2 . The intra-server network topology is a fully connected mesh, while the other topology’s performance bound can be derived in a similar way. Each GPU in the system has a dedicated NIC such that its uplink and downlink bandwidth is B_2 . The transfer size between two different servers i and j is denoted as T_{ij} while the transfer size within server i itself is denoted as S_i . T_{ij} and S_i constitutes the complete All-to-All transfer workload. T_{ii} is meaningless, but we set them to be zero for the ease of writing proofs. We don’t prove the situation where the intra-node transfer is the majority of the All-to-All workload because the nodes can just do the intra-node transfer by themselves, not necessarily be involved in the multi-node communication. So, we assume each server’s intra-node transfer size is not larger than the biggest inter-node transfers, i.e., $S_i \leq \max_{j=0}^{n-1}(T_{ij})$.

THEOREM 1. *The optimal transfer completion time t_{optimal} is:*

$$\frac{1}{mB_2} \max\left(\max_{i=0}^{n-1}\left(\sum_{j=0}^{n-1} T_{ij}\right), \max_{j=0}^{n-1}\left(\sum_{i=0}^{n-1} T_{ij}\right)\right)$$

PROOF. *Let us compute the transfer completion time in an ideal world where the bandwidth of an intra-node network is infinite. The intra-node transfer S_i , load balancing, and data*

redistribution can therefore be instantly completed. After load balancing, each GPU has T_{ij}/m amount of data waiting to be transferred via inter-server links. The inter-server transfers are bound by the largest senders or receivers among all the servers, which is $\max(\max_{i=0}^{n-1} (\sum_{j=0}^{n-1} \frac{T_{ij}}{m}), \max_{j=0}^{n-1} (\sum_{i=0}^{n-1} \frac{T_{ij}}{m}))$. So, the shortest transfer completion time is the value shown in the theorem. Any real-world transfers must be slower or equal to this ideal transfer. \square

THEOREM 2. *FLASH's worst-case transfer completion time t_{FLASH} is:*

$$\begin{aligned} t_{FLASH} = & \frac{1}{mB_2} \max \left(\max_{i=0}^{n-1} \sum_{j=0}^{n-1} T_{ij}, \max_{j=0}^{n-1} \sum_{i=0}^{n-1} T_{ij} \right) \\ & + \frac{1}{mB_1} \max_{i=0}^{n-1} \sum_{j=0}^{n-1} T_{ij} + \frac{1}{B_1} \max_{i,j=0}^{n-1} T_{ij} \quad (1) \\ & + \frac{1}{mB_1} \max_{i,j=0}^{n-1} T_{ij}. \end{aligned}$$

PROOF. We compute FLASH's worst-case performance by summing the longest possible transfer time of each transfer stage. For load balancing, it would take the longest time to complete the job when T_{ij} is located at a single GPU in the beginning, as it causes the largest amount of data (i.e., $(m-1)/m \cdot T_{ij}$) to be balanced. Since the intra-node network is assumed a full mesh, the source GPU can concurrently send T_{ij}/m amount of data to every other GPU via $(m-1)$ directly connected links, making the worst-case load balancing time among the servers as $t_0 = \max_{i=0}^{n-1} (\sum_{j=0}^{n-1} \frac{T_{ij}}{m}) \frac{1}{B_1}$. For the intra-node transfer, the worst case is that all the S_i data is moved between only two GPUs. So, the worst-case time for intra-node transfer is $t_2 = \max_{i=0}^{n-1} \frac{S_i}{B_1} \leq \max_{i=0}^{n-1} \frac{\max_{j=0}^{n-1} (T_{ij})}{B_1} = \max_{i,j=0}^{n-1} \frac{T_{ij}}{B_1}$ by using the assumption $S_i \leq \max_{j=0}^{n-1} (T_{ij})$. For inter-server transfer, Birkhoff's Theorem can generate at most n^2 transfer steps. We first sort them in ascending order based on each step's transfer size and get the sorted size $l_0 \leq l_1 \leq \dots \leq l_{n^2-1}$. We then execute the transfer steps in the sorted order, which successfully hides the current step's data redistribution (lasting l_i/B_1) from the next step's inter-server transfer (lasting l_{i+1}/B_2) since $l_i \leq l_{i+1}$, $B_1 > B_2$. Due to the property of Birkhoff's Theorem, the completion time of inter-node transfer stage t_2 is dividing the size of the largest senders or receivers by the inter-node bandwidth, the same as $t_{optimal}$. Finally, for the last transfer step's data redistribution, the worst case is when the last step transfers the most amount of data, i.e., $\max_{i,j=0}^{n-1} T_{ij}/m$, making the longest completion time as $t_3 = \frac{1}{B_1} \max_{i,j=0}^{n-1} \frac{T_{ij}}{m}$. Therefore, FLASH worst-case transfer time is $t_{FLASH} = t_0 + t_1 + t_2 + t_3$, which is the value shown in the theorem. \square

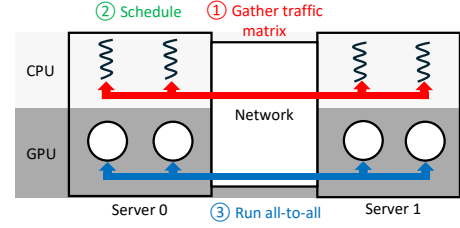


Figure 10: Workflow of FLASH doing online optimization for All-to-All communication in MoE system.

With optimal performance and FLASH's worst-case performance, we can calculate the performance bound.

THEOREM 3. *The gap between FLASH and optimal performance is bound by $\frac{B_2}{B_1} (m+2)$.*

PROOF. We divide FLASH worst-case transfer time by ideal transfer time as follows: $\frac{t_{FLASH}}{t_{optimal}} = \frac{t_0 + t_1 + t_2 + t_3}{t_{optimal}} \leq 1 + \frac{B_2}{B_1} (m+2)$ where we shrink the denominator as follows:

$$\max(\max_{i=0}^{n-1} (\sum_{j=0}^{n-1} T_{ij}), \max_{j=0}^{n-1} (\sum_{i=0}^{n-1} T_{ij})) \geq \max_{i=0}^{n-1} (\sum_{j=0}^{n-1} T_{ij}) \geq \max_{i,j=0}^{n-1} T_{ij}$$

to cancel out the numerator and get the final result. \square

In conclusion, the performance gap is bound by the ratio of intra-server bandwidth to inter-server bandwidth, which means FLASH can be infinitely close to the theoretical optimality given a fast-enough intra-node network.

5 Online Optimizer For MoE System

In this section, we introduce how to integrate FLASH into an MoE training system and show some performance optimization techniques in our implementation.

FLASH does online optimization for every All-to-All communication in MoE training workloads, including All-to-All token dispatching and All-to-All output combining, in both forward and backward passes. As shown in Figure 10, each control thread on the CPU first gathers the traffic matrix from the other threads and then runs a local scheduler to generate a scheduling policy. The local scheduling policies across the threads are consistent because of FLASH's deterministic computation process. Our approach minimizes the scheduling latency because each thread only needs to collect a small traffic matrix while a centralized scheduler must also broadcast the scheduling result. Finally, all the GPUs in the system complete the All-to-All workload according to FLASH's scheduling policy.

We implement FLASH using ROCm [3], NCCL [8] and MSCCL [18] library. We optimize FLASH's performance by applying the following techniques:

(1) *Pipeline the inter- and intra-server transfers:* We put the data into two separate memory regions based on whether it is for inter- or intra-server transfers. We then use two NCCL

communicators and two CUDA/HIP streams to do concurrent inter- and intra-server transfers, building a pipeline shown in Figure 9.

(2) *Avoid data fragmentation after load balancing*: The load balancing in FLASH will cause data fragmentation if the receiver randomly places the incoming load balance data, leading to cache prefetching failures and bad performance in later transfers. We bundle the data having the same destination, whether it is the load balancing data from other GPUs or originally from the current GPU itself, eliminating data fragmentation and allowing for consecutive memory reads.

(3) *Align with GPU cache line size*: We pad the data to the GPU cache line size to further optimize performance. For MI300X GPU with 128-byte cache line [2] we use in our testbed, we pad the transfer size to a multiple of 32 for INT32 and 64 for FP16/BF16.

(4) *Use memcpy for intra-GPU data movement*: When moving data within a GPU, e.g., from the intermediate buffer to the receiving buffer, we use ROCm’s memcpy API instead of NCCL’s send/recv API, as the former is orders-of-magnitude faster.

FLASH hides all its implementation details and exposes a neat Python interface. Existing AI models written in PyTorch can easily deploy FLASH by replacing the default `all_to_all_single` API with FLASH.

6 Evaluation

Our evaluation focuses on the following questions:

- How does FLASH perform compared to baselines across different workloads, transfer sizes, and workload skewness (§6.1)?
- How does FLASH benefit the MoE end-to-end training performance (§6.2)?
- What is FLASH’s performance at larger scales and under varying intra-server topologies and network bandwidths (§6.3)?
- What are the overheads of FLASH (§6.4)?

Testbed. We evaluate FLASH on a 4-node cluster, as shown in Figure 11, with each node containing 8 AMD Instinct MI300X GPUs [2]. Within each node, GPUs are fully connected via AMD Infinity Fabric, with each link providing 64 GBps duplex bandwidth. Each GPU is also equipped with a dedicated 100 Gbps NIC (i.e., 12.5 GBps duplex bandwidth), connected to a Top-of-Rack (ToR) switch. We use commercial ConnectX-6 NICs, which support GPU Direct RDMA [5] and use RoCEv2. The FLASH scheduler runs on AMD EPYC 9534 @2.45 GHz CPUs in each server.

Workload. We evaluate FLASH with both synthetic and real MoE workloads. Our synthetic workloads include:

- **Balanced**: Each GPU sends an equal amount of data to all others, as in prior work.

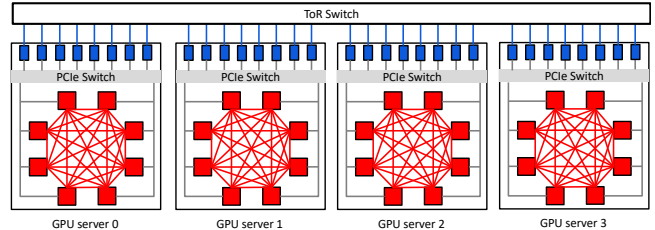


Figure 11: Evaluation testbed. A red/blue rectangle represents a GPU/NIC, while red/blue/grey lines indicate Infinity Fabric, Ethernet, and PCIe links, respectively.

- **Random**: Each GPU sends a varying amount of data, and the transfer size follows a uniform distribution.
- **Skewed**: Some GPUs send significantly more data, with the transfer size following a Zipfian distribution.

For real workloads, we run MoE models using Megatron-LM [49] and measure end-to-end performance gains with FLASH.

6.1 Benchmark Study

Following prior works [4, 48], we evaluate FLASH using *algorithmic bandwidth*, defined as the total transfer size divided by the number of GPUs and the transfer completion time. This metric reflects the average data transfer speed per GPU.

We compare FLASH against four baseline algorithms:

- TACCL [48], a state-of-the-art scheduler that generates optimal communication schedules using Mixed Integer Linear Programming (MILP) based on topology and workload.
- MSCCL [18], a hierarchical algorithm where each GPU first gathers data from GPUs in the same node before sending aggregated data to peer GPUs across nodes.
- RCCL [8], where each GPU transmits to all other GPUs simultaneously.
- MPI [41], that uses the spread-out algorithm operating in multiple phases where each GPU receives from only one sender per phase.

6.1.1 Performance Under Different Transfer Sizes

As shown in Figure 12a, under the balanced workload, FLASH achieves algorithmic bandwidth comparable to MSCCL, ranging from 0.91× to 1×, 1.1× to 91×, and 1.3× to 2.5× that of TACCL, RCCL, and MPI, respectively. With FLASH, TACCL, and MSCCL, intra-server transfers are fully pipelined and hidden behind inter-server transfers, making the total transfer time determined solely by inter-server bandwidth. Thus, they all perform close to the optimal bandwidth, computed as: $\frac{\text{Total transfer size}}{\# \text{ of GPUs}} / (\frac{\text{Inter-server transfer size}}{\text{Inter-server bandwidth}})$, which equates to approximately 15 GBps under the balanced workload in our 4-node testbed. In particular, FLASH attains 14.7 GBps for large transfer sizes, reaching 98% of the optimal performance.

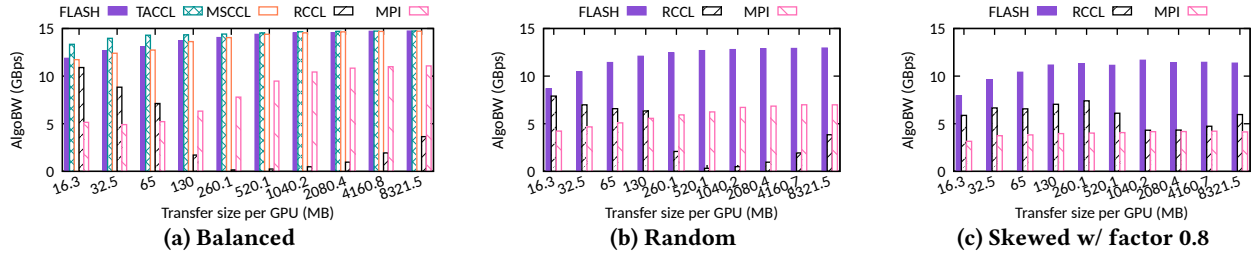


Figure 12: FLASH versus baselines at different transfer sizes under different workloads.

In contrast, RCCL suffers from severe performance degradation due to incast, and MPI Spread-out is bounded by inter-server bandwidth, resulting in lower performance. In MPI Spread-out, although some intra-node transfers complete early, they must wait for the straggler inter-node transfers from the same step, leading to a bottleneck at the inter-server bandwidth limit.

While TACCL performs well under balanced workloads, it struggles with unbalanced workloads. Adapting TACCL’s scheduler—designed for balanced workloads with already-slow computation speed—to unbalanced and skewed scenarios introduces excessive computational overhead, rendering it impractical. Therefore, we exclude TACCL from further comparisons.

As shown in Figure 12b and Figure 12c, under random workloads, FLASH outperforms RCCL and MPI by 1.1–39.6× and 1.9–2.1×, respectively. Under skewed workloads, FLASH achieves 1.4–2.7× and 2.5–2.7× higher bandwidth compared to RCCL and MPI. While RCCL continues to suffer from incast, the impact is somewhat mitigated in unbalanced workloads due to reduced collision frequency and shorter collision duration. In contrast, MPI Spread-out performs significantly worse under unbalanced workloads, as varying transfer sizes further delay the completion of stragglers, exacerbating the straggler effect.

For small transfer sizes (e.g., <130 MB), FLASH exhibits increasing performance with size. This is because FLASH introduces intermediate transfer stages such as load balancing and redistribution, which incur fixed latencies (e.g., memory copies to prevent data fragmentation). These latencies are more pronounced for small transfers but become negligible as transfer sizes grow. In contrast, RCCL exhibits the opposite trend: it starts all transfers immediately without intermediate stages. While small transfers benefit from switch queuing buffers absorbing incast, RCCL’s performance degrades rapidly when the incast exceeds buffer capacity.

6.1.2 Performance Under Different Skewness

We also evaluate the performance by adjusting the skewness factor in the Zipfian distribution. Higher skewness reduces the number of flows while increasing the size of elephant flows, leading to greater workload imbalance. As shown

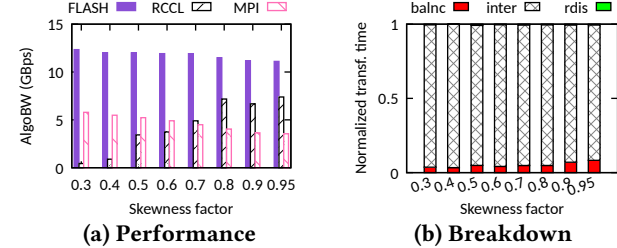


Figure 13: FLASH performance and transfer time breakdown under different-skewed workloads.

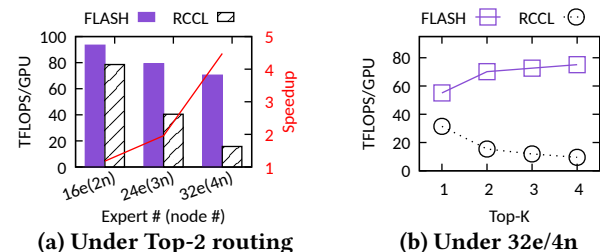


Figure 14: Megatron-LM MoE training performance under varying degree of expert parallelism and Top-K.

in Figure 13a, FLASH achieves 1.6–28× and 2.1–3.1× higher bandwidth compared to RCCL and MPI, respectively.

Unlike FLASH and MPI, RCCL benefits from increased skewness because fewer active transfers reduce the degree of incast. For FLASH, higher skewness results in a longer load-balancing phase (see Figure 13b), delaying the subsequent inter-server transfer stage and leading to temporary bandwidth underutilization. However, since load balancing constitutes only a small fraction of the total transfer time, FLASH maintains strong overall performance. In contrast, MPI suffers from more pronounced straggler effects with increased skewness, leading to further performance degradation.

6.2 End-to-End Performance

To evaluate FLASH in an end-to-end MoE training process, we integrate it into Megatron-LM[49], a transformer training framework, and optimize every All-to-All communication in the MoE model. The baseline is PyTorch’s [39] default `all_to_all_single` method, which employs the RCCL fanout algorithm.

Varying degree of expert parallelism. We benchmark FLASH across different degrees of expert parallelism. Each GPU hosts one expert, similar to DeepSeek [19], while we vary the number of experts (and servers accordingly).

As shown in Figure 14a, training performance (left y-axis) decreases as the number of experts increases. This is expected as more experts require additional nodes and inter-node transfers, slowing All-to-All communication and increasing GPU idle time. The baseline deteriorates significantly as the incast degree increases—with 16 experts, a receiving GPU (NIC) handles at most 8 simultaneous data streams from other nodes, but with 32 experts, this rises to 24. Despite this trend, FLASH achieves 1.18–4.48× speedup in end-to-end training performance over the baseline.

In practical large-language model training, expert counts can be much higher—e.g., 320 in DeepSeek[19] and 2K in GShard[26]—exacerbating the incast issue. In our 32-expert test, RCCL’s All-to-All communication time is about an order of magnitude longer than FLASH—exceeding even GPU computation time!

Varying Top-K routing policy. Next, we evaluate FLASH under different routing policies in a fixed 4-server scenario. In MoE, Top-K directly influences All-to-All workload size, as each input is replicated and sent to the top-K most relevant experts for computation.

As shown in Figure 14b, FLASH and RCCL exhibit opposite performance trends. For FLASH, increasing K enlarges the All-to-All workload, improving performance by amortizing static overhead, similar in observation to Figure 12. For RCCL, however, a larger workload increases the likelihood of send collisions and incast, degrading All-to-All communication and increasing GPU idle time. As a result, with a Top-4 routing policy, FLASH achieves 7.88× the training performance of the baseline. For a fixed expert count, other factors that influence All-to-All workload size, such as batch size, sequence length, and data type size, affect the training performance in a similar way as Top-K.

6.3 Simulation Study

We use simulation to evaluate FLASH at a larger scale and under different intra-server topologies and inter-server bandwidths. Our simulation follows the $\alpha-\beta$ model ([29, 48]), where the transfer time is estimated as the sum of multiple

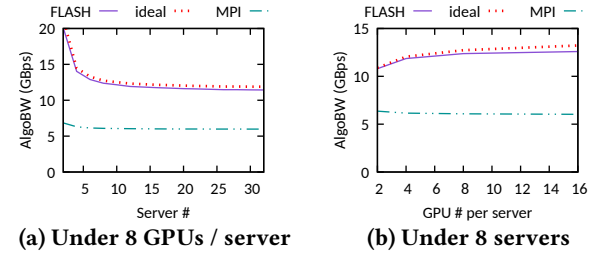


Figure 15: Simulation of large-scale deployment with 100 Gbps RoCE v2 and 900 GBps 4th-gen NVLink under random workload.

small transfers. Each transfer consists of a static link wake-up time (α cost), and a dynamic transmission time (β cost), determined by dividing the data size by the link bandwidth.

6.3.1 Performance At Larger Scales

We evaluate FLASH at scale by varying both the number of servers and the number of GPUs per server. We consider a setup with a 100 Gbps RoCEv2 inter-server network and a 4th-gen NVSwitch fabric [6], offering 900 GBps bidirectional bandwidth per GPU.

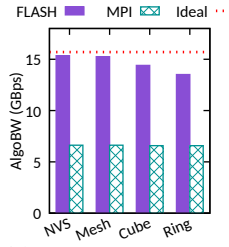
We first examine the impact of scaling the number of servers when each server contains 8 GPUs. As shown in Figure 15a, FLASH achieves near-optimal performance, closely following the theoretical limit. This is because FLASH efficiently balances data using fast intra-server bandwidth before transferring it at full rate over inter-server links. In contrast, MPI spread-out achieves only about half the performance of FLASH due to straggler effects. As the number of servers grows, algorithmic bandwidth declines, and inter-server communication increasingly becomes the bottleneck. With more servers, the fraction of slow inter-server transfers increases, causing performance to converge toward inter-server bandwidth limits.

We also vary the number of GPUs per server in an 8-server cluster. As shown in Figure 15b, FLASH performance increases with more GPUs per server, as a larger fraction of data transfers occurs within high-speed intra-server links. Compared to MPI, FLASH achieves 2× the performance and approaches optimal throughput. While the gap between FLASH and the theoretical optimum slightly widens with more GPUs per server—due to increased load balancing and data redistribution overhead—this gap remains under 9%, even with 16 GPUs per server.

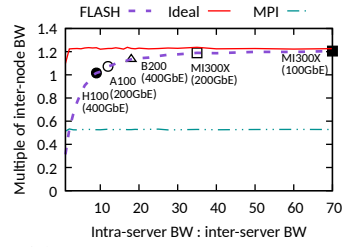
6.3.2 Performance Across Topologies And Bandwidths

We simulate FLASH performance under different intra-server topologies: NVSwitch (H100 [36]), full-mesh (MI300X [2]), ring (MI250X [1]), and hybrid-cube (V100 [34]).

As shown in Figure 16a, FLASH achieves 0.86–0.92× optimal performance under ring and hybrid-cube topologies,



(a) Varying topology



(b) Varying bandwidth ratios

Figure 16: Simulation of different intra-node topology and network bandwidths ($4n \times 8$ GPUs) under random workload.

where the low and asymmetric GPU connectivity increases the cost for data shuffling and redistribution. In contrast, FLASH reaches near-optimal performance in switch and full-mesh topologies—the more common intra-server GPU fabric architecture favoring FLASH. MPI spread-out is not sensitive to the intra-server GPU topology as it is usually slowed by the stragglers using inter-server links.

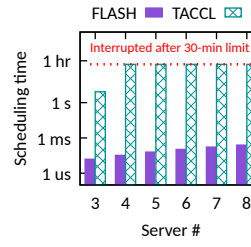
We also examine FLASH performance under varying intra- and inter-server bandwidths, simulating different GPU models paired with different RoCE network speeds. As shown in Figure 16b, the performance improves as the ratio of intra-server to inter-server bandwidth increases, as faster intra-server links accelerate data shuffling and redistribution. For instance, with B200 GPUs [35] paired with 400 Gbps NICs, FLASH achieves $0.92 \times$ optimal performance. The growth of intra-server bandwidth is likely to outpace inter-server due to their scales, further favoring FLASH over time.

6.4 System Overhead

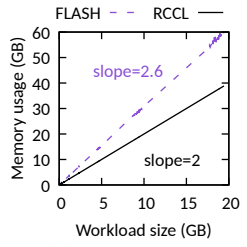
FLASH introduces two types of overhead compared to baseline systems: (1) time for scheduling computation and (2) memory for intermediate transfer stages.

FLASH’s scheduling time is negligible relative to the reduction in transfer time, leading to overall performance gains. Figure 17a shows scheduling time under random workloads with 3 servers, where FLASH completes scheduling in $\approx 15 \mu\text{s}$, while reducing transfer completion time by over 2500 μs for per-GPU transfer sizes above 100 MB. For comparison, Figure 17a also presents the scheduling time of TACCL [48], which relies on computation-heavy Mixed Integer Linear Programming (MILP). We manually terminate TACCL’s scheduler if it exceeds 30 minutes. Unlike TACCL, which is suited for static workloads, FLASH performs efficient online optimization, making it more adaptable to dynamic workloads such as MoE.

Regarding memory overhead, FLASH incurs $\approx 30\%$ additional memory usage than RCCL or MPI. Figure 17b shows the relationship between memory footprint and workload size under random workloads. The baseline’s slope is 2, as



(a) Scheduling time



(b) Memory usage

Figure 17: System overhead under random workload.

each workload byte requires one byte in the sending buffer and one in the receiving buffer. FLASH has a slope of ≈ 2.6 , with additional memory used for intermediate stages such as load balancing and data redistribution.

7 Related Work

FLASH is related to a rich body of prior work that optimizes collective communications [4, 8, 13, 14, 18, 29, 41, 46, 48, 52]. The MPI library [41] has proposed many efficient implementations of collective communications, including Spread-out and Bruke algorithm [33] for All-to-All transfers. However, these prior works assume homogeneous interconnects between computation nodes, failing to fully utilize the heterogeneous networks in modern GPU clusters. NCCL [4] and RCCL [8] address this inefficiency by using high-bandwidth intra-server GPU interconnects such as NVLink to accelerate inter-GPU communications. But their All-to-All algorithm is unaware of possible congestion in the inter-node network, suffering from incast at large scales. Recent work such as SCCL [14], TACCL [48], and TE-CCL [29] models the complete topology of GPU interconnects and different link bandwidth to generate near-optimal scheduling using SMT, MILP, and traffic engineering solver. However, their computation cost is extremely high and impractical to deploy in real applications. FLASH abstracts away the concrete topologies of GPU interconnects but simply classifies them as a fast and slow network. By using the intra-node fast network to maximize the utilization of the slow inter-node network, FLASH achieves near-optimal performance with negligible overhead.

FLASH is also relevant to the work that optimizes the mixture-of-expert model [19, 21, 24–27, 44]. Many work like deepspeed-MoE [44] optimizes the model structure, such as altering the number of experts and Top-K routing decisions. Other work such as Lina [27] and Tutel [24] exploits the pipelining of computation and All-to-All communication. Orthogonal to the prior work, FLASH focuses on optimizing the bottleneck, i.e., the unbalanced and dynamic All-to-All workload, to improve the MoE performance.

Besides, FLASH is related to prior work [15, 28] that uses Birkhoff’s Theorem [12] to schedule packet switching in

the router crossbar. FLASH applies the theorem to solve a different problem that optimizes the All-to-All collective communication.

8 Conclusion

All-to-All communication is the performance key to many applications such as mixture-of-expert models. Existing works that optimize All-to-All communication either have poor performance due to their failures to handle incast or stragglers or incur highly-expensive computation. This paper presents FLASH, an All-to-All scheduling system that achieves near-optimal performance with negligible scheduling overhead. Our key idea is abstracting the GPU interconnects into a fast and slow network and maximizing the performance of the bottleneck inter-node network with the help of the fast intra-node network. We evaluate FLASH in a MoE training task and find it can improve the MoE training performance up to 4.5× in a 4-node cluster.

This work does not raise any ethical issues.

References

- [1] [n. d.]. AMD CDNA2 Architecture. ([n. d.]). <https://www.amd.com/content/dam/amd/en/documents/instinct-business-docs/white-papers/amd-cdna2-white-paper.pdf>.
- [2] [n. d.]. AMD CDNA3 Architecture. ([n. d.]). <https://www.amd.com/content/dam/amd/en/documents/instinct-tech-docs/white-papers/amd-cdna-3-white-paper.pdf>.
- [3] [n. d.]. AMD ROCm. ([n. d.]). <https://github.com/ROCM/ROCM>.
- [4] [n. d.]. NVIDIA Collective Communications Library (NCCL). ([n. d.]). <https://developer.nvidia.com/nccl>.
- [5] [n. d.]. NVIDIA GPUDirect. ([n. d.]). <https://developer.nvidia.com/gpudirect>.
- [6] [n. d.]. NVLink & NVSwitch. ([n. d.]). <https://www.nvidia.com/en-us/data-center/nvlink/>.
- [7] [n. d.]. RCCL FanOut All-to-All Algorithm. ([n. d.]). <https://github.com/ROCM/rccl/blob/develop/src/collectives.cc>.
- [8] [n. d.]. ROCm Communication Collectives Library (RCCL). ([n. d.]). <https://github.com/ROCM/rccl>.
- [9] Alan Ayala, Stanimir Tomov, Xi Luo, Hejer Shaeik, Azzam Haidar, George Bosilca, and Jack Dongarra. 2019. Impacts of Multi-GPU MPI Collective Communications on Large FFT Computation. In *2019 IEEE/ACM Workshop on Exascale MPI (ExaMPI)*. 12–18. <https://doi.org/10.1109/ExaMPI49596.2019.00007>
- [10] Prithwish Basu, Liangyu Zhao, Jason Fantl, Siddharth Pal, Arvind Krishnamurthy, and Joud Khoury. 2024. Efficient All-to-All Collective Communication Schedules for Direct-Connect Topologies. (2024). arXiv:cs.DC/2309.13541 <https://arxiv.org/abs/2309.13541>
- [11] H.J.C. Berendsen, D. van der Spoel, and R. van Drunen. 1995. GROMACS: A message-passing parallel molecular dynamics implementation. *Computer Physics Communications* 91, 1 (1995), 43–56. [https://doi.org/10.1016/0010-4655\(95\)00042-E](https://doi.org/10.1016/0010-4655(95)00042-E)
- [12] Garrett Birkhoff. 1946. Three observations on linear algebra. *Univ. Nac. Tucumán. Revista A.* 5 (1946), 147–151.
- [13] NVIDIA Blog. 2022. NVIDIA Rail-optimized topology. (2022). <https://developer.nvidia.com/blog/doubling-all2all-performance-with-nvidia-collective-communication-library-2-12/>.
- [14] Zixian Cai, Zhengyang Liu, Saeed Maleki, Madanlal Musuvathi, Todd Mytkowicz, Jacob Nelson, and Olli Saarikivi. 2021. Synthesizing optimal collective algorithms. In *Proceedings of the 26th ACM SIGPLAN Symposium on Principles and Practice of Parallel Programming*. ACM. <https://doi.org/10.1145/3437801.3441620>
- [15] Cheng-Shang Chang, Wen-Jyh Chen, and Hsiang-Yi Huang. 2000. Birkhoff-von Neumann input buffered crossbar switches. In *Proceedings IEEE INFOCOM 2000. Conference on Computer Communications. Nineteenth Annual Joint Conference of the IEEE Computer and Communications Societies (Cat. No.00CH37064)*, Vol. 3. 1614–1623 vol.3. <https://doi.org/10.1109/INFCOM.2000.832560>
- [16] Mosharaf Chowdhury and Ion Stoica. 2012. Coflow: a networking abstraction for cluster applications. In *Proceedings of the 11th ACM Workshop on Hot Topics in Networks (HotNets-XI)*. Association for Computing Machinery, New York, NY, USA, 31–36. <https://doi.org/10.1145/2390231.2390237>
- [17] Ultra Ethernet Consortium. 2023. *Overview of and Motivation for the Forthcoming Ultra Ethernet Consortium Specification*. Technical Report.
- [18] Meghan Cowan, Saeed Maleki, Madanlal Musuvathi, Olli Saarikivi, and Yifan Xiong. 2023. MSCCLang: Microsoft Collective Communication Language. In *Proceedings of the 28th ACM International Conference on Architectural Support for Programming Languages and Operating Systems, Volume 2 (ASPLOS 2023)*. Association for Computing Machinery, New York, NY, USA, 502–514. <https://doi.org/10.1145/3575693.3575724>
- [19] DeepSeek-AI, Aixin Liu, Bei Feng, Bing Xue, Bingxuan Wang, Bochao Wu, Chengda Lu, Chenggang Zhao, Chengqi Deng, Chenyu Zhang, Chong Ruan, Damai Dai, Daya Guo, Dejian Yang, Deli Chen, Dongjie Ji, Erhang Li, Fangyun Lin, Fucong Dai, Fuli Luo, Guangbo Hao, Guanting Chen, Guowei Li, H. Zhang, Han Bao, Hanwei Xu, Haocheng Wang, Haowei Zhang, Honghui Ding, Huajian Xin, Huazuo Gao, Hui Li, Hui Qu, J. L. Cai, Jian Liang, Jianzhong Guo, Jiaqi Ni, Jiashi Li, Jiawei Wang, Jin Chen, Jingchang Chen, Jingyang Yuan, Junjie Qiu, Junlong Li, Junxiao Song, Kai Dong, Kai Hu, Kaige Gao, Kang Guan, Kexin Huang, Kuai Yu, Lean Wang, Lecong Zhang, Lei Xu, Leyi Xia, Liang Zhao, Litong Wang, Liyue Zhang, Meng Li, Miaojun Wang, Mingchuan Zhang, Minghua Zhang, Minghui Tang, Mingming Li, Ning Tian, Panpan Huang, Peiyi Wang, Peng Zhang, Qiancheng Wang, Qihao Zhu, Qinyu Chen, Qiushi Du, R. J. Chen, R. L. Jin, Ruiqi Ge, Ruisong Zhang, Ruizhe Pan, Runji Wang, Runxin Xu, Ruoyu Zhang, Ruyi Chen, S. S. Li, Shanghao Lu, Shangyan Zhou, Shanhua Chen, Shaoqing Wu, Shengfeng Ye, Shengfeng Ye, Shirong Ma, Shiyu Wang, Shuang Zhou, Shuiping Yu, Shunfeng Zhou, Shuting Pan, T. Wang, Tao Yun, Tian Pei, Tianyu Sun, W. L. Xiao, Wangding Zeng, Wanja Zhao, Wei An, Wen Liu, Wenfeng Liang, Wenjun Gao, Wenqin Yu, Wentao Zhang, X. Q. Li, Xiangyue Jin, Xianzu Wang, Xiao Bi, Xiaodong Liu, Xiaohan Wang, Xiaojin Shen, Xiaokang Chen, Xiaokang Zhang, Xiaosha Chen, Xiaotao Nie, Xiaowen Sun, Xiaoxiang Wang, Xin Cheng, Xin Liu, Xin Xie, Xingchao Liu, Xingkai Yu, Xinnan Song, Xinxia Shan, Xinyi Zhou, Xinyu Yang, Xinyuan Li, Xuecheng Su, Xuheng Lin, Y. K. Li, Y. Q. Wang, Y. X. Wei, Y. X. Zhu, Yang Zhang, Yanhong Xu, Yanhong Xu, Yanping Huang, Yao Li, Yao Zhao, Yaofeng Sun, Yaohui Li, Yaohui Wang, Yi Yu, Yi Zheng, Yichao Zhang, Yifan Shi, Yiliang Xiong, Ying He, Ying Tang, Yishi Piao, Yisong Wang, Yixuan Tan, Yiyang Ma, Yiyuan Liu, Yongqiang Guo, Yu Wu, Yuan Ou, Yuchen Zhu, Yuduan Wang, Yue Gong, Yuheng Zou, Yujia He, Yukun Zha, Yunfan Xiong, Yunxian Ma, Yuting Yan, Yuxiang Luo, Yuxiang You, Yuxuan Liu, Yuyang Zhou, Z. F. Wu, Z. Z. Ren, Zehui Ren, Zhangli Sha, Zhe Fu, Zhean Xu, Zhen Huang, Zhen Zhang, Zhenda Xie, Zhengyan Zhang, Zhewen Hao, Zhibin Gou, Zhicheng Ma, Zhigang Yan, Zhihong Shao, Zhipeng Xu, Zhiyu Wu, Zhongyu Zhang, Zhuoshu Li, Zihui Gu, Zijia Zhu, Zijun Liu, Zilin Li, Ziwei Xie, Ziyang Song, Ziyi Gao, and Zizheng Pan. 2024. DeepSeek-V3 Technical Report. (2024). arXiv:cs.CL/2412.19437

https://arxiv.org/abs/2412.19437

[20] Fanny Dufossé and Bora Uçar. 2016. Notes on Birkhoff–von Neumann decomposition of doubly stochastic matrices. *Linear Algebra Appl.* 497 (2016), 108–115. <https://doi.org/10.1016/j.laa.2016.02.023>

[21] William Fedus, Barret Zoph, and Noam Shazeer. 2022. Switch Transformers: Scaling to Trillion Parameter Models with Simple and Efficient Sparsity. (2022). arXiv:cs.LG/2101.03961 <https://arxiv.org/abs/2101.03961>

[22] Adithya Gangidi, Rui Miao, Shengbao Zheng, Sai Jayesh Bondu, Guilherme Goes, Hany Morsy, Rohit Puri, Mohammad Riftadi, Ashmitha Jeevaraj Shetty, Jingyi Yang, Shuqiang Zhang, Mikel Jimenez Fernandez, Shashidhar Gandham, and Hongyi Zeng. 2024. RDMA over Ethernet for Distributed Training at Meta Scale. In *Proceedings of the ACM SIGCOMM 2024 Conference (ACM SIGCOMM '24)*. Association for Computing Machinery, New York, NY, USA, 57–70. <https://doi.org/10.1145/3651890.3672233>

[23] Yixiao Gao, Yuchen Yang, Tian Chen, Jiaqi Zheng, Bing Mao, and Guihai Chen. 2018. DCQCN+: Taming Large-Scale Incast Congestion in RDMA over Ethernet Networks. In *2018 IEEE 26th International Conference on Network Protocols (ICNP)*. 110–120. <https://doi.org/10.1109/ICNP.2018.00021>

[24] Changho Hwang, Wei Cui, Yifan Xiong, Ziyue Yang, Ze Liu, Han Hu, Zilong Wang, Rafael Salas, Jithin Jose, Prabhat Ram, Joe Chau, Peng Cheng, Fan Yang, Mao Yang, and Yongqiang Xiong. 2023. Tutel: Adaptive Mixture-of-Experts at Scale. (2023). arXiv:cs.DC/2206.03382 <https://arxiv.org/abs/2206.03382>

[25] Albert Q. Jiang, Alexandre Sablayrolles, Antoine Roux, Arthur Mensch, Blanche Savary, Chris Bamford, Devendra Singh Chaplot, Diego de las Casas, Emma Bou Hanna, Florian Bressand, Gianna Lengyel, Guillaume Bour, Guillaume Lample, Lélio Renard Lavaud, Lucile Saulnier, Marie-Anne Lachaux, Pierre Stock, Sandeep Subramanian, Sophia Yang, Szymon Antoniak, Teven Le Scao, Théophile Gervet, Thibaut Lavril, Thomas Wang, Timothée Lacroix, and William El Sayed. 2024. Mixtral of Experts. (2024). arXiv:cs.LG/2401.04088 <https://arxiv.org/abs/2401.04088>

[26] Dmitry Lepikhin, HyoukJoong Lee, Yuanzhong Xu, Dehao Chen, Orhan Firat, Yanping Huang, Maxim Krikun, Noam Shazeer, and Zhifeng Chen. 2020. GShard: Scaling Giant Models with Conditional Computation and Automatic Sharding. (2020). arXiv:cs.CL/2006.16668 <https://arxiv.org/abs/2006.16668>

[27] Jiamin Li, Yimin Jiang, Yibo Zhu, Cong Wang, and Hong Xu. 2023. Accelerating Distributed MoE Training and Inference with Lina. In *2023 USENIX Annual Technical Conference (USENIX ATC 23)*. USENIX Association, Boston, MA, 945–959. <https://www.usenix.org/conference/atc23/presentation/li-jiamin>

[28] He Liu, Matthew K. Mukerjee, Conglong Li, Nicolas Feltman, George Papen, Stefan Savage, Srinivasan Seshan, Geoffrey M. Voelker, David G. Andersen, Michael Kaminsky, George Porter, and Alex C. Snoeren. 2015. Scheduling techniques for hybrid circuit/packet networks. In *Proceedings of the 11th ACM Conference on Emerging Networking Experiments and Technologies (CoNEXT '15)*. Association for Computing Machinery, New York, NY, USA, Article 41, 13 pages. <https://doi.org/10.1145/2716281.2836126>

[29] Xuting Liu, Behnaz Arzani, Siva Kesava Reddy Kakarla, Liangyu Zhao, Vincent Liu, Miguel Castro, Srikanth Kandula, and Luke Marshall. 2024. Rethinking Machine Learning Collective Communication as a Multi-Commodity Flow Problem. In *Proceedings of the ACM SIGCOMM 2024 Conference (ACM SIGCOMM '24)*. Association for Computing Machinery, New York, NY, USA, 16–37. <https://doi.org/10.1145/3651890.3672249>

[30] Parviz Moin and Krishnan Mahesh. 1998. Direct Numerical Simulation: A Tool in Turbulence Research. *Annu. Rev. Fluid Mech.* 30 (01 1998), 539–578. <https://doi.org/10.1146/annurev.fluid.30.1.539>

[31] Dheevatsa Mudigere, Yuchen Hao, Jianyu Huang, Zhihao Jia, Andrew Tulloch, Srinivas Sridharan, Xing Liu, Mustafa Ozdal, Jade Nie, Jong-soo Park, Liang Luo, Jie Amy Yang, Leon Gao, Dmytro Ivchenko, Aarti Basant, Yuxi Hu, Jiyuan Yang, Ehsan K. Ardestani, Xiaodong Wang, Rakesh Komuravelli, Ching-Hsiang Chu, Serhat Yilmaz, Huayu Li, Jiyuan Qian, Zhuobo Feng, Yinbin Ma, Junjie Yang, Ellie Wen, Hong Li, Lin Yang, Chonglin Sun, Whitney Zhao, Dimitry Melts, Krishna Dhulipala, KR Kishore, Tyler Graf, Assaf Eisenman, Kiran Kumar Matam, Adi Gangidi, Guoqiang Jerry Chen, Manoj Krishnan, Avinash Nayak, Krishnakumar Nair, Bharath Muthiah, Mahmoud khorashadi, Pallab Bhattacharya, Petr Lapukhov, Maxim Naumov, Ajit Mathews, Lin Qiao, Mikhail Smelyanskiy, Bill Jia, and Vijay Rao. 2023. Software-Hardware Co-design for Fast and Scalable Training of Deep Learning Recommendation Models. (2023). arXiv:cs.DC/2104.05158 <https://arxiv.org/abs/2104.05158>

[32] Maxim Naumov, John Kim, Dheevatsa Mudigere, Srinivas Sridharan, Xiaodong Wang, Whitney Zhao, Serhat Yilmaz, Changkyu Kim, Hector Yuen, Mustafa Ozdal, Krishnakumar Nair, Isabel Gao, Bor-Yiing Su, Jiyuan Yang, and Mikhail Smelyanskiy. 2020. Deep Learning Training in Facebook Data Centers: Design of Scale-up and Scale-out Systems. (2020). arXiv:cs.DC/2003.09518 <https://arxiv.org/abs/2003.09518>

[33] Naeris Netterville, Ke Fan, Sidharth Kumar, and Thomas Gilray. 2022. A Visual Guide to MPI All-to-all. In *2022 IEEE 29th International Conference on High Performance Computing, Data and Analytics Workshop (HiPCW)*. 20–27. <https://doi.org/10.1109/HiPCW57629.2022.00008>

[34] NVIDIA. 2017. NVidia V100 GPU Architecture. (2017). <https://images.nvidia.com/content/volta-architecture/pdf/volta-architecture-whitepaper.pdf>

[35] NVIDIA. 2025. NVidia B200 GPU Datasheet. (2025). <https://resources.nvidia.com/en-us-dgx-systems/dgx-b200-datasheet?ncid=no-ncid>

[36] NVIDIA. 2025. NVidia H100 GPU Architecture. (2025). <https://resources.nvidia.com/en-us-tensor-core>

[37] Johan Obando-Ceron, Ghada Sokar, Timon Willi, Clare Lyle, Jesse Farebrother, Jakob Foerster, Gintare Karolina Dziugaite, Doina Precup, and Pablo Samuel Castro. 2024. Mixtures of Experts Unlock Parameter Scaling for Deep RL. (2024). arXiv:cs.LG/2402.08609 <https://arxiv.org/abs/2402.08609>

[38] OpenAI, Josh Achiam, Steven Adler, Sandhini Agarwal, Lama Ahmad, Ilge Akkaya, Florencia Leoni Aleman, Diogo Almeida, Janko Altenschmidt, Sam Altman, Shyamal Anadkat, Red Avila, Igor Babuschkin, Suchir Balaji, Valerie Balcom, Paul Baltescu, Haiming Bao, Mohammad Bavarian, Jeff Belgum, Irwan Bello, Jake Berdine, Gabriel Bernadett-Shapiro, Christopher Berner, Lenny Bogdonoff, Oleg Boiko, Madelaine Boyd, Anna-Luisa Brakman, Greg Brockman, Tim Brooks, Miles Brundage, Kevin Button, Trevor Cai, Rosie Campbell, Andrew Cann, Brittany Carey, Chelsea Carlson, Rory Carmichael, Brooke Chan, Che Chang, Fotis Chantzis, Derek Chen, Sully Chen, Ruby Chen, Jason Chen, Mark Chen, Ben Chess, Chester Cho, Casey Chu, Hyung Won Chung, Dave Cummings, Jeremiah Currier, Yunxing Dai, Cory Decareaux, Thomas Degry, Noah Deutsch, Damien Deville, Arka Dhar, David Dohan, Steve Dowling, Sheila Dunning, Adrien Ecoffet, Atty Eleti, Tyna Eloundou, David Farhi, Liam Fedus, Niko Felix, Simón Posada Fishman, Juston Forte, Isabella Fulford, Leo Gao, Elie Georges, Christian Gibson, Vik Goel, Tarun Gogineni, Gabriel Goh, Rapha Gontijo-Lopes, Jonathan Gordon, Morgan Grafstein, Scott Gray, Ryan Greene, Joshua Gross, Shixiang Shane Gu, Yufei Guo, Chris Hallacy, Jesse Han, Jeff Harris, Yuchen He, Mike Heaton, Johannes Heidecke, Chris Hesse, Alan Hickey, Wade Hickey, Peter Hoeschele, Brandon Houghton, Kenny Hsu, Shengli Hu, Xin Hu, Joost Huizinga, Shantanu Jain, Shawn Jain, Joanne Jang, Angela Jiang, Roger Jiang, Haozhen Jin, Denny Jin, Shino Jomoto, Billie Jonn, Heewoo Jun, Tomer

Kaftan, Łukasz Kaiser, Ali Kamali, Ingmar Kanitscheider, Nitish Shirish Keskar, Tabarak Khan, Logan Kilpatrick, Jong Wook Kim, Christina Kim, Yongjik Kim, Jan Hendrik Kirchner, Jamie Kiros, Matt Knight, Daniel Kokotajlo, Łukasz Kondraciuk, Andrew Kondrich, Aris Konstantinidis, Kyle Kosic, Gretchen Krueger, Vishal Kuo, Michael Lampe, Ikai Lan, Teddy Lee, Jan Leike, Jade Leung, Daniel Levy, Chak Ming Li, Rachel Lim, Molly Lin, Stephanie Lin, Mateusz Litwin, Theresa Lopez, Ryan Lowe, Patricia Lue, Anna Makanju, Kim Malfacini, Sam Manning, Todor Markov, Yaniv Markovski, Bianca Martin, Katie Mayer, Andrew Mayne, Bob McGrew, Scott Mayer McKinney, Christine McLeavey, Paul McMillan, Jake McNeil, David Medina, Aalok Mehta, Jacob Menick, Luke Metz, Andrey Mishchenko, Pamela Mishkin, Vinnie Monaco, Evan Morikawa, Daniel Mossing, Tong Mu, Mira Murati, Oleg Murk, David Mély, Ashvin Nair, Reiichiro Nakano, Rajeev Nayak, Arvind Nee-lakantan, Richard Ngo, Hyeonwoo Noh, Long Ouyang, Cullen O'Keefe, Jakub Pachocki, Alex Paino, Joe Palermo, Ashley Pantuliano, Giambattista Parascandolo, Joel Parish, Emy Parparita, Alex Passos, Mikhail Pavlov, Andrew Peng, Adam Perelman, Filipe de Avila Belbute Peres, Michael Petrov, Henrique Ponde de Oliveira Pinto, Michael, Pokorny, Michelle Pokrass, Vitchyr H. Pong, Tolly Powell, Alethea Power, Boris Power, Elizabeth Proehl, Raul Puri, Alec Radford, Jack Rae, Aditya Ramesh, Cameron Raymond, Francis Real, Kendra Rimbach, Carl Ross, Bob Rotsted, Henri Roussez, Nick Ryder, Mario Saltarelli, Ted Sanders, Shibani Santurkar, Girish Sastry, Heather Schmidt, David Schnurr, John Schulman, Daniel Selsam, Kyla Sheppard, Toki Sherbakov, Jessica Shieh, Sarah Shoker, Pranav Shyam, Szymon Sidor, Eric Sigler, Maddie Simens, Jordan Sitkin, Katarina Slama, Ian Sohl, Benjamin Sokolowsky, Yang Song, Natalie Staudacher, Felipe Petroski Such, Natalie Summers, Ilya Sutskever, Jie Tang, Nikolas Tezak, Madeleine B. Thompson, Phil Tillet, Amin Tootoonchian, Elizabeth Tseng, Preston Tuggle, Nick Turley, Jerry Tworek, Juan Felipe Cerón Uribe, Andrea Vallone, Arun Vijayvergiya, Chelsea Voss, Carroll Wainwright, Justin Jay Wang, Alvin Wang, Ben Wang, Jonathan Ward, Jason Wei, CJ Weinmann, Akila Welihinda, Peter Welinder, Jiayi Weng, Lilian Weng, Matt Wiethoff, Dave Willner, Clemens Winter, Samuel Wolrich, Hannah Wong, Lauren Workman, Sherwin Wu, Jeff Wu, Michael Wu, Kai Xiao, Tao Xu, Sarah Yoo, Kevin Yu, Qiming Yuan, Wojciech Zaremba, Rowan Zellers, Chong Zhang, Marvin Zhang, Shengjia Zhao, Tianhao Zheng, Juntang Zhuang, William Zhuk, and Barret Zoph. 2024. GPT-4 Technical Report. (2024). arXiv:cs.CL/2303.08774 <https://arxiv.org/abs/2303.08774>

[39] Adam Paszke, Sam Gross, Francisco Massa, Adam Lerer, James Bradbury, Gregory Chanan, Trevor Killeen, Zeming Lin, Natalia Gimelshein, Luca Antiga, Alban Desmaison, Andreas Köpf, Edward Yang, Zach DeVito, Martin Raison, Alykhan Tejani, Sasank Chilamkurthy, Benoit Steiner, Lu Fang, Junjie Bai, and Soumith Chintala. 2019. PyTorch: An Imperative Style, High-Performance Deep Learning Library. (2019). arXiv:cs.LG/1912.01703 <https://arxiv.org/abs/1912.01703>

[40] Dmitry Pekurovsky. 2012. P3DFFT: A Framework for Parallel Computations of Fourier Transforms in Three Dimensions. *SIAM Journal on Scientific Computing* 34, 4 (Jan. 2012), C192–C209. <https://doi.org/10.1137/11082748x>

[41] J. Pjesivac-Grbovic, T. Angskun, G. Bosilca, G.E. Fagg, E. Gabriel, and J.J. Dongarra. 2005. Performance analysis of MPI collective operations. In *19th IEEE International Parallel and Distributed Processing Symposium*. 8 pp.–. <https://doi.org/10.1109/IPDPS.2005.335>

[42] Bogdan Prisacari, German Rodriguez, Cyriel Minkenberg, and Torsten Hoefer. 2013. Bandwidth-optimal all-to-all exchanges in fat tree networks. In *Proceedings of the 27th International ACM Conference on International Conference on Supercomputing (ICS '13)*. Association for Computing Machinery, New York, NY, USA, 139–148. <https://doi.org/10.1145/2464996.2465434>

[43] Sarunya Pumma and Abhinav Vishnu. 2021. Semantic-Aware Lossless Data Compression for Deep Learning Recommendation Model (DLRM). In *2021 IEEE/ACM Workshop on Machine Learning in High Performance Computing Environments (MLHPC)*. 1–8. <https://doi.org/10.1109/MLHPC54614.2021.00006>

[44] Samyam Rajbhandari, Conglong Li, Zhewei Yao, Minjia Zhang, Reza Yazdani Aminabadi, Ammar Ahmad Awan, Jeff Rasley, and Yuxiong He. 2022. DeepSpeed-MoE: Advancing Mixture-of-Experts Inference and Training to Power Next-Generation AI Scale. (2022). arXiv:cs.LG/2201.05596 <https://arxiv.org/abs/2201.05596>

[45] Carlos Riquelme, Joan Puigcerver, Basil Mustafa, Maxim Neumann, Rodolphe Jenatton, André Susano Pinto, Daniel Keysers, and Neil Houlsby. 2021. Scaling Vision with Sparse Mixture of Experts. (2021). arXiv:cs.CV/2106.05974 <https://arxiv.org/abs/2106.05974>

[46] Daniele De Sensi, Tommaso Bonato, David Saam, and Torsten Hoefer. 2024. Swing: Short-cutting Rings for Higher Bandwidth Allreduce. In *21st USENIX Symposium on Networked Systems Design and Implementation (NSDI 24)*. USENIX Association, Santa Clara, CA, 1445–1462. <https://www.usenix.org/conference/nsdi24/presentation/de-sensi>

[47] Alexander Sergeev and Mike Del Balso. 2018. Horovod: fast and easy distributed deep learning in TensorFlow. (2018). arXiv:cs.LG/1802.05799 <https://arxiv.org/abs/1802.05799>

[48] Aashaka Shah, Vijay Chidambaram, Meghan Cowan, Saeed Maleki, Madan Musuvathi, Todd Mytkowicz, Jacob Nelson, Olli Saarikivi, and Rachee Singh. 2022. TACCL: Guiding Collective Algorithm Synthesis using Communication Sketches. (2022). arXiv:cs.DC/2111.04867 <https://arxiv.org/abs/2111.04867>

[49] Mohammad Shoeybi, Mostofa Patwary, Raul Puri, Patrick LeGresley, Jared Casper, and Bryan Catanzaro. 2020. Megatron-LM: Training Multi-Billion Parameter Language Models Using Model Parallelism. (2020). arXiv:cs.CL/1909.08053 <https://arxiv.org/abs/1909.08053>

[50] Vijay Vasudevan, Amar Phanishayee, Hiral Shah, Elie Krevat, David G. Andersen, Gregory R. Ganger, Garth A. Gibson, and Brian Mueller. 2009. Safe and effective fine-grained TCP retransmissions for datacenter communication. In *Proceedings of the ACM SIGCOMM 2009 Conference on Data Communication (SIGCOMM '09)*. Association for Computing Machinery, New York, NY, USA, 303–314. <https://doi.org/10.1145/1592568.1592604>

[51] Vijay Vasudevan, Amar Phanishayee, Hiral Shah, Elie Krevat, David G. Andersen, Gregory R. Ganger, Garth A. Gibson, and Brian Mueller. 2009. Safe and effective fine-grained TCP retransmissions for datacenter communication. In *Proceedings of the ACM SIGCOMM 2009 Conference on Data Communication (SIGCOMM '09)*. Association for Computing Machinery, New York, NY, USA, 303–314. <https://doi.org/10.1145/1592568.1592604>

[52] Guanhua Wang, Shivaram Venkataraman, Amar Phanishayee, Jorgen Thelin, Nikhil R. Devanur, and Ion Stoica. 2019. Blink: Fast and Generic Collectives for Distributed ML. *CoRR* abs/1910.04940 (2019). arXiv:1910.04940 <http://arxiv.org/abs/1910.04940>